RSC Advances

PAPER

View Article Online
View Journal | View Issue

Cite this: *RSC Adv.*, 2025, **15**, 4526

Heterobifunctional cross-linker with dinitroimidazole and azide modules for protein and oligonucleotide functionalization†

Qunfeng Luo, * Shuli Liu, Yaoguang Hua, Chunqiu Long, Sijia lv, Juncheng Li and Yuzhi Zhang

Received 10th November 2024
Accepted 20th January 2025

DOI: 10.1039/d4ra07987f

rsc.li/rsc-advances

Dinitroimidazole (DNIm) was recently identified as a powerful bioconjugation agent that could selectively modify thiol over amine on biomolecules at an ultrahigh speed in an aqueous buffer. However, its derivative containing a DNIm module and a terminal alkyne module failed to construct functional agents bearing a DNIm warhead *via* the CuAAC reaction. To solve this problem, a heterobifunctional cross-linker was designed and synthesized by linking a DNIm module with an azide module *via* an oxoaliphatic amido bond spacer arm. Its two modules, DNIm and azide, reacted with a thiol and cyclooctyne, respectively, in an orthogonal way. The cross-linker facilitated the preparation of various functional agents bearing a DNIm warhead *via* SPAAC reaction and was further applied to protein functionalization (including biotinylation and fluorescence labeling) and oligonucleotide functionalization (including PEGylation, oligonucleotide–peptide and oligonucleotide–protein conjugate). Thus, the cross-linker not only provided convenient access to those functional agents bearing a DNIm warhead but also combined DNIm chemistry with click chemistry of SPAAC to enlarge their respective application range in the bioconjugation field.

Introduction

Heterobifunctional cross-linkers comprise two different reactive modules connected by a linker chain. There are many such reactive modules, such as *N*-hydroxysuccinimide (NHS)[1,2] (**1c**; Fig. 1A), maleimide (**1a**),[3] the α-haloacetamide group[4] (**1b**), alkynyl groups (**1a**, **1b**, **1e**),[4] azide group (**1c**)[4] and recently developed dinitroimidazole (**1e**).[5] Cross-linkers are the centerpiece of bioconjugation chemistry for development of peptide- or antibody–drug conjugates[6,7] and therapeutic oligonucleotide drugs.[8]

The strain-promoted alkyne azide cycloaddition (SPAAC) is an outstanding reaction in the bioorthogonal conjugation field owing to its splendid chemical stability, non-toxicity, mild reaction conditions, and high efficiency.[9] SPAAC reaction utilizes two reaction modules, namely, azide and cyclooctyne groups. Many research groups have focused on expanding the pool of cyclooctynes and enhancing their reactivity toward azides. So far, the most commonly used cyclooctynes are dibenzocyclooctyne (DBCO)[10] and bicyclononyne (BCN)[11] owing to their relatively simple synthesis with sufficient yield and great coupling efficiency.

Recently, it was identified that dinitroimidazole (DNIm) could selectively modify a thiol over an amine on biomolecules at an ultrahigh speed in an aqueous buffer.[5] DNIm and its thiol adduct generated *via* bioconjugation were extremely stable

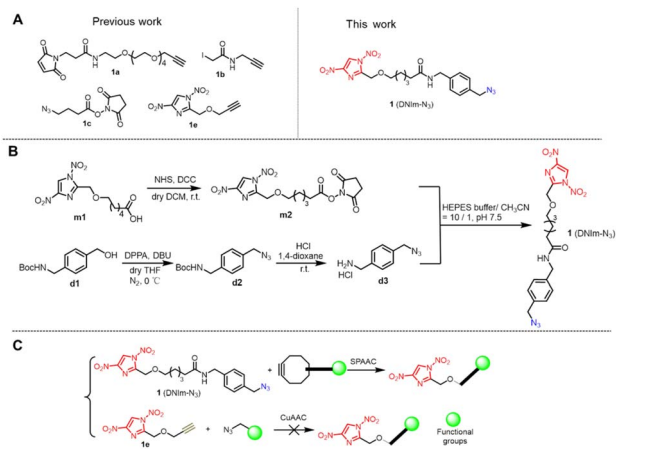

Fig. 1 (A) Chemical structures of heterobifunctional cross-linkers from previous work and this work. (B) Chemical synthesis of DNIm-N_3. (C) SPAAC reaction between the cross-linker **1** and cyclooctynes generated functional agents bearing a DNIm warhead, but CuAAC reaction between **1e** and azides failed to.

School of Basic Medical Sciences, Jiangxi Medical College, Nanchang University, Nanchang, Jiangxi 330006, People's Republic of China. E-mail: luoqunfeng@ncu.edu.cn

† Electronic supplementary information (ESI) available. See DOI: https://doi.org/10.1039/d4ra07987f

under tested conditions. DNIm revealed a few superiorities in stability and water solubility aspects compared to those of the maleimide and perfluoroaryl reagents. Besides, the adduct core fragment thiol-(4-nitroimidazole) was harmless to 293T cells under 10 μM, which endowed it with great potential to be utilized in live cells or pharmaceutical development. Considering these advantages, DNIm is promising to be a valuable addition to the current bioconjugation toolbox.

We envisioned combining DNIm chemistry with click chemistry of SPAAC to enlarge their respective application range in the bioconjugation field. With this in mind, we tried to incorporate two components (DNIm and azide group) into one to generate heterobifunctional cross-linker **1** (DNIm-N_3) *via* an oxoaliphatic amido bond spacer arm (Fig. 1). Although a similar cross-linker containing DNIm and terminal alkyne modules has been reported[5] (**1e**; Fig. 1A), it has failed to construct functional agents bearing a DNIm warhead *via* the CuAAC reaction (Fig. 1C and ESI Fig. 7†) resulting in the destruction of DNIm. We speculate that side reactions might happen owing to the additives in the click reaction mixture, such as copper, sodium ascorbate and THPTA. If the side reaction results from copper, it is rational and necessary to design and synthesize cross-linker **1**, which employs copper-free SPAAC chemistry, which could overcome the obstacle existing in **1e**. Furthermore, the azide group in **1** endows it with more power in bioconjugation owing to the reaction versatility of azides.[12] Notably, we only focused on the SPAAC reaction in this work.

Results and discussion

CuAAC reaction between cross-linker 1e and d2

A model reaction of CuAAC was conducted by incubating compounds **1e** and **d2** (an azide, Fig. 1B) under routine conditions, $CuSO_4$/VcNa/THPTA in this work (ESI Fig. 7†). Compound **1e** (1 mM) and azide **d2** (1 mM) were dissolved in neutral HEPES buffer (50 mM). Then, $CuSO_4$ (1 mM), THPTA (1 mM) and VcNa (2 mM) were added successively. The cycloaddition product **ed2** was formed in high yield as showed by HPLC analysis, but lost one –NO_2 group at the N1 position of the imidazole ring, which was confirmed by HRMS and NMR data (ESI Fig. 8†). The detailed mechanism for the formation of the side product **ed2** is still under exploration. In other words, the CuAAC reaction between **1e** and azide failed to generate functional agents bearing a DNIm warhead, which prompted us to probe other alternative approaches to achieve this goal.

Design and chemical synthesis of cross-linker DNIm-N_3

As is known, organic azides are potentially explosive substances that decompose with the release of nitrogen through the slightest input of external energy, for example, pressure, impact, or heat. Those manipulable or nonexplosive organic azides conform to the rule that the number of nitrogen atoms must not exceed that of carbon and that $(N_C + N_O)/N_N \geq 3$ (N = number of atoms).[13] On the other hand, considering the reported synthetic route to various DNIm derivatives and the commercial availability of azide materials, we decided to synthesize cross-linker **1**.

The key precursor **m1** was synthesized first referring to the reported method.[5] Next, compound **m1** was condensed with NHS in the presence of DCC in dry DCM to afford compound **m2** confirmed by HRMS and NMR in 74% yield. Compound **m2** has two reaction modules, the DNIm module for sulfhydryl, and the NHS ester module for amine. Compound **d3** containing an amine group and an azide group was designed to react with the NHS ester module of compound **m2**. To obtain compound **d3**, compound **d1** was mixed with DPPA and DBU in dry THF under an N_2 atmosphere and 0 °C to give compound **d2** in which the hydroxyl group in **d1** was replaced with an azide group. Then, compound **d2** was treated with HCl in 1,4-dioxane solution to release the amine group to afford compound **d3**. Lastly, compound **m2** was mixed with compound **d3** in slightly basal HEPES buffer, which afforded the desired compound **1** as confirmed by HRMS and NMR in 89% yield (Fig. 1B and ESI Fig. 1–6†).

Orthogonal reaction of DNIm and azide modules in DNIm-N_3 with Cys and (DBCO or BCN) derivatives

With the cross-linker **1** in hand, we then tested its reaction characteristics with Cys and (BCN or DBCO) derivatives. We started with the reaction between cross-linker **1** and L-cysteine **c1**. In neutral HEPES buffer, cross-linker **1** reacted with **c1** to give the desired product **mc1** identified by HPLC and HRMS (Fig. 2A and ESI Fig. 9†). Byproduct **2** was also observed with a 19% percentage in which the –NO_2 group at the N1 position was lost compared to that in **1**. **c2** is a pentapeptide with amino acid sequence CWHKM containing one free cysteine residue and was chosen to react with cross-linker **1** (Fig. 2A). In the same condition as that between **1** and **c1**, only DNIm module in **1** reacted with the sulfhydryl group in peptide **c2** to give compound **mc2** in high yield as confirmed by HPLC and HRMS (Fig. 2A and ESI Fig. 9†).

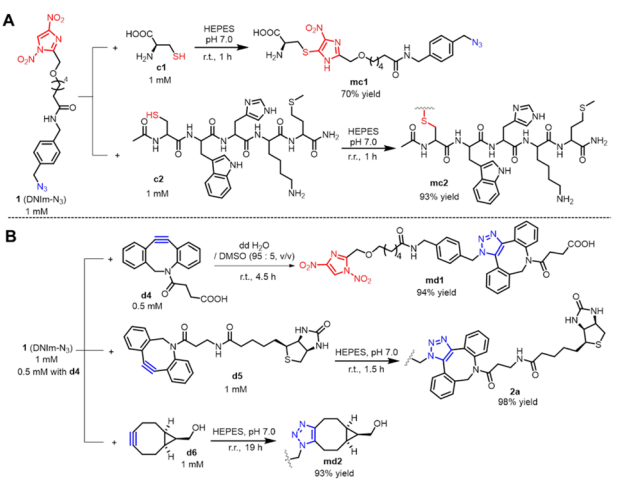

Fig. 2 Orthogonal reaction of DNIm and azide modules in DNIm-N_3 with Cys and (DBCO or BCN) derivatives: (A) reaction of DNIm module with Cys; (B) reaction of the azide module with DBCO or BCN derivatives.

Then, we explored the reaction of cross-linker **1** with DBCO or BCN derivatives. In an aqueous solution with 5% DMSO; incubation of the cross-linker **1** with **d4** for 4.5 h at r. t. produced the desired product **md1** as determined by HPLC and HRMS. However, the HPLC spectrum presented two adjacent peaks with nearly the same integral area, which may be attributed to two regioisomeric triazoles formed in approximately equal amounts as reported by Agard *et al.*[14] (Fig. 2B and ESI Fig. 10†). Another DBCO derivative bearing a biotin group, **d5** was adopted to react with cross-linker **1**. In neutral HEPES buffer, after 1.5 h of stirring, the desired product **2a** formed nearly quantitatively as shown by HPLC and HRMS (Fig. 2B, ESI Fig. 11A and C†). To further explore the orthogonality between the azide module in DNIm-N_3 and the DBCO group, incubation of compound DNIm with **d4** in neutral HEPES buffer was performed. The reaction proceeded for 52 h at r. t. and no product was formed as demonstrated by HPLC analysis, which convinced us that DNIm did not interfere with the reaction between the azide module and the DBCO group (ESI Fig. 11B and D†). Likewise, BCN derivative **d6** was stirred with cross-linker **1** in neutral HEPES buffer to give the title compound **md2** in high yield (Fig. 2B and ESI Fig. 12†). Briefly, DNIm and azide modules in cross-linker **1** demonstrated good orthogonality toward Cys and cyclooctyne derivatives (DBCO and BCN), respectively, which makes it a good heterobifunctional cross-linker.

Preparation of functional agents bearing a DNIm warhead with DNIm-N_3 *via* SPAAC reaction

The orthogonal reaction characteristics of the two modules in cross-linker **1** prompted us to utilize it to modify proteins. Attaching various functionalities, such as fluorophore and biotin, to proteins is valuable in the fields of biomedical research.[15] We initiated this application by preparing several functional agents (**3a**, **4a**, and **5a**; Fig. 3) bearing a DNIm warhead for Cys modification. To obtain compound **3a**, the intermediate BCN-biotin was prepared first through acylation of biotin-NH_2 by compound BCN-NHS in a weakly basal methanol solution. Then, the incubation of compound BCN-biotin with cross-linker **1** in neutral HEPES buffer produced compound **3a** *via* the SPAAC reaction in high yields as determined by HPLC analysis and HRMS (Fig. 3 and ESI Fig. 13†). Likewise, to obtain compound **4a**, the intermediate BCN-dansyl was synthesized first through acylation of dansyl-NH_2 by compound BCN-NHS (Fig. 3 and ESI Fig. 14†). Then, the incubation of compound BCN-dansyl with cross-linker **1** in MeOH produced compound **4a** *via* SPAAC reaction. Before being applied to protein bioconjugation, the solvent MeOH was removed in a vacuum. Nearly in the same synthetic route as in **4a**; compound furazan–NH_2 was condensed with BCN-NHS to form the intermediate BCN-furazan, which further proceeded through the reaction of SPAAC with DNIm-N_3 to give compound **5a** (Fig. 3 and ESI Fig. 15†). All the functional agents **3a**, **4a** and **5a** were applied directly for biomolecule modification without further purification.

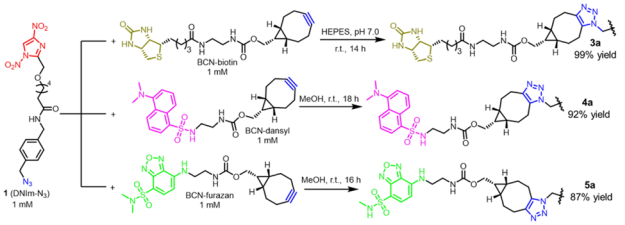

Fig. 3 Preparation of functional agents bearing a dinitroimidazole warhead with cross-linker **1** *via* the SPAAC reaction.

Modification of protein by functional dinitroimidazole agents bearing biotin or fluorescence group

As is known, the binding affinity of biotin to streptavidin is one of the highest reported for non-covalent interactions to date, with $K_D \sim 0.01$ pM. Thus, biotinylation is widely used in biotechnological fields, such as protein purification[16] and drug target fishing.[17] In this work, the biotin group was incorporated into the cross-linker **1** to generate functional molecules **2a** and **3a** near quantitatively (Fig. 2B, 3, ESI Fig. 11 and 13†). Bovine serum albumin (BSA) was chosen as a model protein. It contains one free cysteine (Cys34) and 59 lysines. Treatment of BSA with compound **2a** or **3a** for 1–2 h in a neutral buffer successfully

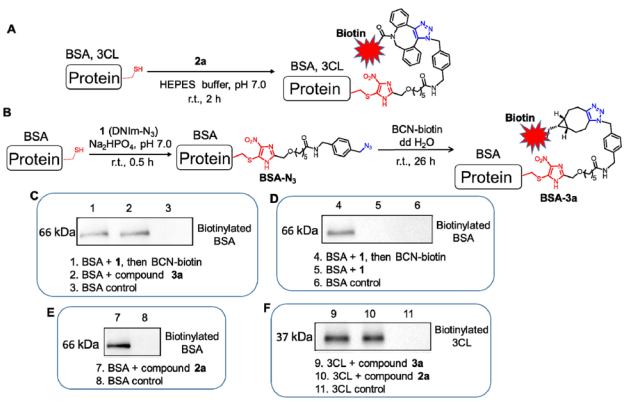

Fig. 4 Modification of protein by functional dinitroimidazole agents bearing the biotin group. (A) Reaction scheme for BSA and 3CL modified by compound **2a**; (B) reaction scheme for BSA modified by DNIm-N_3 and BCN-biotin successively. BSA was modified by DNIm-N_3 first to attach an azide group to BSA, followed by linking to the BCN-biotin *via* SPAAC reaction; (C) western blot analysis of biotinylated BSA. Lane 1: BSA + **1**, then BCN-biotin. Conditions (refer to (B)): incubation of 30 μM of BSA with 60 μM of DNIm-N_3 in a neutral Na_2HPO_4 buffer for 0.5 h. Then, the excess DNIm-N_3 was removed through PD MiniTrap™ G-25 columns (Cytiva). The intermediate (15 μM) was then mixed with BCN-biotin (30 μM) in dd H_2O for 26 h to produce the biotinylated BSA bioconjugate. Lane 2: BSA + compound **3a**. Conditions: incubation of 35 μM of BSA with 285 μM of compound **3a** in phosphate buffer at pH 7.0. (D) Western blot analysis of biotinylated BSA. Lane 4: BSA + **1**, then BCN-biotin. Conditions: refer to lane 1 in (C). Lane 5: BSA + **1**. Conditions: refer to the first step of lane 4. (E) Western blot analysis of biotinylated BSA by compound **2a**. Lane 7: BSA + compound **2a**. Conditions: BSA (30 μM), compound **2a** (120 μM), 3% DMSO. (F) Western blot analysis of biotinylated 3CL by compound **2a** or **3a**. Lane 9: 3CL + compound **3a**. Conditions: 3CL (30 μM), compound **3a** (400 μM). Lane 10: 3CL + compound **2a**. Conditions: 3CL (30 μM), compound **2a** (240 μM), 3% DMSO. The uncropped versions for (C–F) are available in ESI Fig. 21.†

attached the biotin group to BSA as determined by western blot analysis (Fig. 4A, C, E, and 6A) and LC-MS (Fig. 5E and F). Notably, in Fig. 5F, a minor product of BSA doubly modified by **2a** was detected (**BSA-2a***), one at –SH, another at $–NH_2$. It might result from the organic solvent DMSO added in the solution (Fig. 4E), since we have reported that in a neutral aqueous buffer, DNIm attacks –SH rather than $–NH_2$, however, in organic solution, DNIm attacks $–NH_2$ at a high rate.[5] Also, the remaining high concentration of the labelling reagent (**2a**) might bring about the unexpected modification at $–NH_2$. In comparison with the experiment in lane 2 of Fig. 4C, BSA was treated with cross-linker **1** and compound BCN-biotin, successively (Fig. 4C lane 1, Fig. 4D lane 4 and lane 5, Fig. 4B). The desired protein bands were also observed by western blot analysis and the molecular weight of the two bioconjugates (**BSA-N_3**, **BSA-3a**) were confirmed by LC-MS (Fig. 5B and C), although the minor amount of BSA remained. All the biotinylation on BSA showed a high conversion rate as determined by the software Thermo Scientific BioPharmaFinder™ 5.3 (Fig. 5; F3. Data analysis, 2. Experimental procedures in the ESI file†). Similarly, 3CL was also selected as a model protein for biotinylation. 3CL used in this work is a variant of the main protease (Mpro) of SARS-COV-2 with Ser46 changed to Phe (S46F), and a purification tag with 33 amino acids was added at its N terminal. It is composed of 339 amino acids and contains twelve free cysteines and eleven lysines, while only three cysteines are exposed to the solvent.[18] Incubation of 3CL with compound **2a** or **3a** for 1 h also generated the biotinylated products as demonstrated by western blot data (Fig. 4A, F, and 6A). Unexpectedly, the two bioconjugates soon precipitated after desalting using the PD MiniTrap™ G-25 column, and therefore no signal of mass spectroscopy was detected in the supernatant.

Then, we tested the activity of functional DNIm agents bearing the fluorescence group. Compound **4a** contains a dansyl fluorophore that can be efficiently excited by ultraviolet (UV) light,[19] while 302 nm light was used in this work. Incubation of 3CL with compound **4a** for 1 h in neutral phosphate buffer

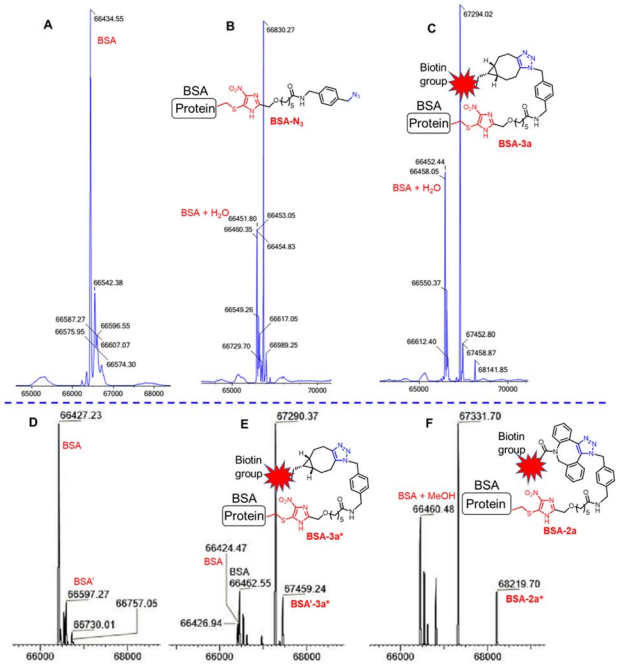

Fig. 5 Deconvoluted mass spectrum of BSA and its bioconjugates. (A) Deconvoluted mass spectrum of BSA. Mass for BSA: Calc. 66 429.98 Da, Obs. 66 434.55 Da. (B) Deconvoluted mass spectrum of **BSA-N3** that formed by the modification of BSA by DNIm-N_3 with a conversion rate of 89.2%. Mass for conjugate **BSA-N_3**, Calc. 66 829.15 Da, Obs. 66 830.27 Da. The hydrate of BSA was also detected as shown in the mass spectrum: BSA + H_2O, Calc. 66 447.99 Da, Obs. 66 451.80 Da. (C) Deconvoluted mass spectrum of **BSA-3a** formed by the modification of BSA by **1** and BCN-biotin, successively. Mass for **BSA-3a**: Calc. 67 291.38 Da, Obs. 67 294.02 Da. The conversion rate for the step (from **BSA-N_3** to **BSA-3a**) is 100%. Mass for the hydrate of BSA (BSA + H_2O): Calc. 66 447.99 Da, Obs. 66 452.44 Da. (D) Deconvoluted mass spectrum of BSA in another test. Mass for BSA: Calc. 66 429.98 Da, Obs. 66 427.23 Da. BSA′ (66 597.27) is a gradient with low abundance in the sample. (E) Deconvoluted mass spectrum of **BSA-3a*** formed by the modification of BSA by **3a** with a conversion rate of 96.6%. Mass for **BSA-3a*** Calc. 67 291.38 Da, Obs. 67 290.37 Da. Theoretically, **BSA-3a*** and **BSA-3a** (C) are the same ones with identical molecular weights. The mass signal 67 459.24 (**BSA′-3a***) is also a reasonable adduct formed by the modification of BSA′ (66 597.27, (D)) by **3a**. Mass for **BSA′-3a***: Calc. 67 458.67 Da, Obs. 67 459.24 Da. When calculating the conversion rate, it was also included. (F) Deconvoluted mass spectrum of **BSA-2a** formed by the modification of BSA by **2a** with a conversion rate of 83.7%. Mass for **BSA-2a**: Calc. 67 331.35 Da, Obs. 67 331.70 Da. The mass signal 68 219.70 (**BSA-2a***) is the product of BSA doubly modified by **2a**, one at –SH, another at $–NH_2$. When calculating the conversion rate, the single-modified and dual-modified products were considered as a whole. Mass for **BSA-2a***: Calc. 68 217.71 Da, Obs. 68 219.70 Da. Mass for methanol adduct of BSA (BSA + MeOH): Calc. 66 459.26 Da, Obs. 66 460.48 Da.

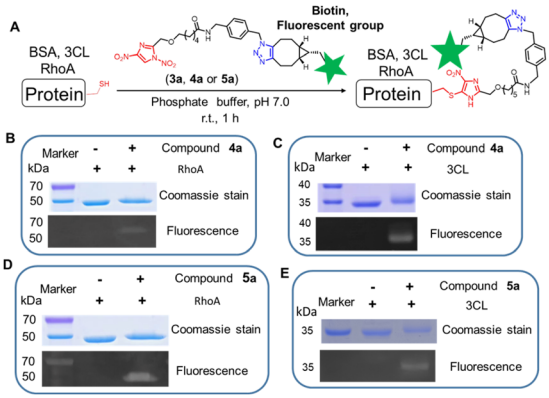

Fig. 6 Modification of protein by functional dinitroimidazole molecules bearing biotin or a fluorescent group. All the fluorescence images were converted to black and white. (A) Bioconjugation of protein by functional dinitroimidazole derivatives. (B) SDS-PAGE analysis of the fluorescent labeling of RhoA by compound **4a**. Conditions: RhoA (18 μM), compound **4a** (100 μM), 5% DMSO. The fluorescence was irradiated at 302 nm. (C) SDS-PAGE analysis of the fluorescent labeling of 3CL by compound **4a**. Condition: 3CL (25 μM), compound **4a** (100 μM), 5% DMSO. (D) SDS-PAGE analysis of the fluorescent labeling of RhoA by compound **5a**. Condition: RhoA (16 μM), compound **5a** (50 μM), 5% DMSO. The fluorescence was irradiated with blue light (440–485 nm). (E) SDS-PAGE analysis of the fluorescent labeling of 3CL by compound **5a**. Conditions: 3CL (30 μM), compound **5a** (100 μM), and 3% DMSO.

resulted in strong fluorescent labelling compared to that in the control in which **4a** was not added (Fig. 6C and ESI Fig. 18C†). RhoA is a fusion protein that is composed of 422 amino acids and contains 10 cysteine residues and 38 lysine residues[20] and was also selected as a model protein. 18 μM RhoA was mixed with 100 μM compound **4a** for 1 h in neutral buffer. Sodium dodecyl sulfate-polyacrylamide gel electrophoresis (SDS-PAGE) analysis and irradiation with 302 nm light demonstrated evident fluorescence (Fig. 6B and ESI Fig. 18A†). Inspired by the labelling effect of compound **4a**, we then designed compound **5a** (Fig. 3) bearing a benzofurazan skeleton that is suitable to be excited with visible light at 450 nm.[21] Incubation of RhoA with compound **5a** in a neutral buffer formed the desired fluorescent band demonstrated by SDS-PAGE analysis and irradiation with blue light (440–485 nm) (Fig. 6D and ESI Fig. 18B†). 3CL was also applied to explore the modification power of compound **5a**. 3CL was treated with compound **5a** in a neutral buffer for 1 h affording a bright band excited by blue light (Fig. 6E and ESI Fig. 18D†). Unfortunately, we did not obtain the mass spectra of the four samples due to precipitation after desalting.

When carrying out protein expression and purification, precipitation is a common issue. In bioconjugation chemistry, new tags are attached to the protein, which may change the active spatial structure and induce precipitation. Though precipitation prevented us from obtaining mass spectra of partial bioconjugation products, SDS-PAGE and western blot analysis manifested the desired products. Overall, cross-linker **1** enabled us to perform facile functionalization of protein using dinitroimidazole and azide chemistry.

Modification of oligonucleotide by DNIm-N_3

Natural oligonucleotides is polyanionic macromolecules with poor drug-like properties. However, the conjugation of specific molecules to oligonucleotides is a promising approach to developing nucleic acid-based drugs. Over the past two decades, medicinal chemists have identified many conjugation strategies, *e.g.*, conjugation with polyethylene glycol, which can improve the nuclease stability, with antibody, which can improve biodistribution to a specific region or cell type, and/or with cholesterol, which increase lipophilicity.[22] The significance of bioconjugation of oligonucleotides inspired us to probe the applicability of the cross-linker **1** in oligonucleotide modification. An oligonucleotide (**o1**) with 22 bases and one click group DBCO at a 5′ terminal was designed and ordered. Next, **o1** was mixed with cross-linker **1** in neutral HEPES buffer to give the intermediate DNA-D-DNIm *via* SPAAC reaction, followed by the addition of cysteine-containing chemicals, *e.g.*, SH-PEG-OH (2000 Da), peptide **c2** (AcNH-CWHKM-$CONH_2$) and BSA (Fig. 7A). The resulting oligonucleotide-PEG and oligonucleotide–peptide conjugate were analyzed by Urea-PAGE (Fig. 7B, lane 3 and 4) and the data showed that **o1** was successfully conjugated by PEG and peptide in 44% and 47% yield in two reaction steps, respectively, processed using ImageJ. In contrast to the reaction order "**o1** + DNIm-N_3 + BSA" shown in Fig. 7C lane 7, BSA was first conjugated with DNIm-N_3, and subsequently linked to **o1** *via* the SPAAC reaction (Fig. 7C lane 8).

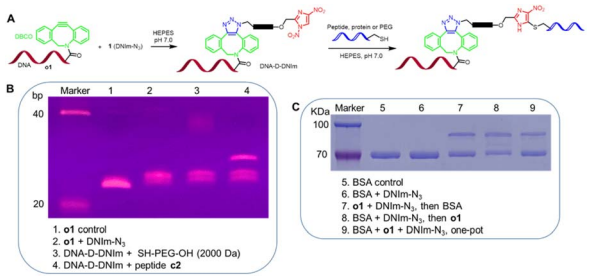

Fig. 7 Modification of the oligonucleotide by cross-linker DNIm-N_3. (A) Reaction scheme for preparation of oligonucleotide conjugates. Oligonucleotide **o1** was first incubated with DNIm-N_3 to attach a DNIm group onto it, then conjugated with cysteine-containing PEG or peptide (protein) *via* DNIm chemistry. Please see Experimental procedures 2C in the ESI file† for detailed profiles of the reaction; (B) Urea-PAGE analysis of oligonucleotide-PEG and oligonucleotide–peptide conjugates; (C) SDS-PAGE analysis of oligonucleotide–BSA conjugate. These five samples (lanes 3, 4, 7, 8 and 9) were quantitatively analyzed by ImageJ (ImageJ 1.52n, Wayne Rasband, National Institutes of Health, USA). Calculation equation: the intensity of the product band/the intensity of the control. The uncropped versions for (B) and (C) are available in ESI Fig. 22.†

Again, we performed a one-pot reaction in which **o1** and BSA were mixed immediately followed by the addition of DNIm-N_3. All these three samples (lanes 7–9 of Fig. 7C) were tested by SDS-PAGE and demonstrated 36%, 47% and 33% yield in two steps, respectively, as analysed using ImageJ. We found that the labelling efficiency on oligonucleotide seemed evidently lower than that on the protein (Fig. 5). However, it is reasonable considering that: first, an equal amount of labelling reagent was used in the reaction with oligonucleotide (Experimental procedures 2C in the ESI file†), while several equivalents of reagents were used for protein; secondly, the yield for oligonucleotide covered two steps, especially one step involving a reaction between two biomacromolecules, while that for protein covered only one.

The conjugate oligonucleotide–peptide in lane 4 of Fig. 7B was confirmed by MALDI-TOF mass analysis (ESI Fig. 19†). Likewise, the conjugate oligonucleotide–BSA in lane 9 of Fig. 7C was confirmed by MALDI-TOF mass analysis. The three samples in lanes 7–9 of Fig. 7C showed the same peak around 74 150, while only one was presented here (ESI Fig. 20†).

Conclusions

We developed a practical heterobifunctional cross-linker bearing two orthogonal reaction modules, namely, DNIm and the azide group. Various functional agents bearing a DNIm warhead were successfully prepared with a cross-linker **1** *via* the SPAAC reaction, which provided us a solution to the side reaction that appeared in the CuAAC reaction of cross-linker **1e**. Therefore, our previous speculation seems reasonable that the presence of copper might be one of the factors that leads to the side reaction. These functional agents were utilized to modify protein, including biotinylation and fluorescence labeling. We also extended the application range to oligonucleotide

functionalization, including PEGylation, oligonucleotide–peptide and oligonucleotide–protein conjugate. Above all, cross-linker **1** was compatible with protein as well as oligonucleotide biomolecules, which makes it a versatile tool for bioconjugation.

Data availability

The data supporting this article have been included as part of the ESI.†

Author contributions

Qunfeng Luo carried out all the chemical synthesis work and prepared the manuscript. Shuli Liu carried out most biochemical experiments. Yaoguang Hua conducted partial biochemical experiments. Chunqiu Long assisted Shuli Liu in completing the biochemical experiments. Juncheng Li and Sijia Lv and Yuzhi Zhang took charge of the picture collection and process.

Conflicts of interest

There are no conflicts to declare.

Acknowledgements

This work was financially supported by the National Natural Science Foundation of China (22007077). The authors gratefully acknowledge the Institute of Biomedical Sciences, Nanchang University, for providing good experimental instruments and equipment. The authors are grateful to the Biomedical Testing Center of Nanchang University and Dr Wuxin You and Prof. Ansgar Poetsch for technical support in corroboration of protein adducts with mass spectrometry. The authors also thank Prof. Jin Zhang (Nanchang University) for supporting the biochemical experiments and Experimentalists Juan Liang and Ye He (Nanchang University) for their help with ultraviolet transmission reflectometry. We also thank Prof. Sai-Sai Xie (Jiangxi University of Traditional Chinese Medicine) for supporting the chemical synthesis experiments and Dr Qi Chen (Nanchang University) for his instructive advice about the usage of horseradish peroxidase-labelled streptavidin.

Notes and references

1 J. Konč, L. Brown, D. R. Whiten, Y. Zuo, P. Ravn, D. Klenerman and G. J. L. Bernardes, *Angew Chem. Int. Ed. Engl.*, 2021, **60**, 25905–25913.
2 G. T. Hermanson, in *Bioconjugate Techniques*, ed. G. T. Hermanson, Academic Press, Boston, 3rd edn, 2013, pp. 299–339, DOI: 10.1016/B978-0-12-382239-0.00006-6.
3 N. L. Kjærsgaard, R. A. Hansen and K. V. Gothelf, *Bioconjugate Chem.*, 2022, **33**, 1254–1260.
4 A. M. ElSohly, J. I. MacDonald, N. B. Hentzen, I. L. Aanei, K. M. El Muslemany and M. B. Francis, *J. Am. Chem. Soc.*, 2017, **139**, 3767–3773.
5 Q. Luo, Y. Tao, W. Sheng, J. Lu and H. Wang, *Nat. Commun.*, 2019, **10**, 142.
6 K. Tsuchikama and Z. An, *Protein Cell*, 2016, **9**, 33–46.
7 M. Alas, A. Saghaeidehkordi and K. Kaur, *J. Med. Chem.*, 2021, **64**, 216–232.
8 T. C. Roberts, R. Langer and M. J. A. Wood, *Nat. Rev. Drug Discovery*, 2020, **19**, 673–694.
9 R. Dudchak, M. Podolak, S. Holota, O. Szewczyk-Roszczenko, P. Roszczenko, A. Bielawska, R. Lesyk and K. Bielawski, *Bioorg. Chem.*, 2023, **143**, 106982.
10 M. F. Debets, S. S. van Berkel, S. Schoffelen, F. P. J. T. Rutjes, J. C. M. van Hest and F. L. van Delft, *Chem. Commun.*, 2010, **46**, 97–99.
11 J. Dommerholt, S. Schmidt, R. Temming, L. J. A. Hendriks, F. P. J. T. Rutjes, J. C. M. van Hest, D. J. Lefeber, P. Friedl and F. L. van Delft, *Angew Chem. Int. Ed. Engl.*, 2010, **49**, 9422–9425.
12 C. I. Schilling, N. Jung, M. Biskup, U. Schepers and S. Bräse, *Chem. Soc. Rev.*, 2011, **40**, 4840–4871.
13 S. Bräse, C. Gil, K. Knepper and V. Zimmermann, *Angew. Chem., Int. Ed.*, 2005, **44**, 5188–5240.
14 N. J. Agard, J. A. Prescher and C. R. Bertozzi, *J. Am. Chem. Soc.*, 2004, **126**, 15046–15047.
15 E. Holz, M. Darwish, D. B. Tesar and W. Shatz-Binder, *Pharmaceutics*, 2023, **15**, 600.
16 J.-N. Rybak, S. B. Scheurer, D. Neri and G. Elia, *Proteomics*, 2004, **4**, 2296–2299.
17 X. Chen, Y. Wang, N. Ma, J. Tian, Y. Shao, B. Zhu, Y. K. Wong, Z. Liang, C. Zou and J. Wang, *Signal Transduction Targeted Ther.*, 2020, **5**, 72.
18 Q. Hu, Y. Xiong, G. H. Zhu, Y. N. Zhang, Y. W. Zhang, P. Huang and G. B. Ge, *MedComm*, 2020, **3**(3), e151.
19 B. Patrascu, S. Mocanu, A. Coman, A. M. Madalan, C. Popescu, A. Paun, M. Matache and P. Ionita, *Int. J. Mol. Sci.*, 2020, **21**, 3559.
20 H. Zhou, X. Yue, Z. Wang, S. Li, J. Zhu, Y. Yang and M. Liu, *Protein Expr. Purif.*, 2021, **180**, 6.
21 T. Santa, *Biomed. Chromatogr.*, 2014, **28**, 760–766.
22 S. Benizri, A. Gissot, A. Martin, B. Vialet, M. W. Grinstaff and P. Barthélémy, *Bioconjug. Chem.*, 2019, **30**, 366–383.